coil, i.e., $C* \approx M^{-4/5}$ (where M is the molecular weight of the macromolecules).[20] But the formation of internal cross-links in a polymer coil means the existence of loops.[20] Theoretical[21,22] studies have shown that in a good solvent where excluded-volume effects predominate, the probability that two given polymer sites on the same chain come into close contact decreases sharply with their distance on the chain. In a polyhydroxy compound–borate system where any polymer site is able to form a complex, intrachain complexes would then imply the existence of small loops whose size should be governed by the local structure of the chain (i.e., rigidity). In this "small loop" picture, the concentration of complexes is independent of the polymer molecular weight (as far as the chain is longer than a possible minimal loop length). Still the number of intrachain complexes per macromolecule increases with the molecular weight. As a consequence, for polyhydroxy compound solutions we may expect that intrachain borate complex formation is more easy for flexible polymers such as poly(vinyl alcohol) or poly(glyceryl methacrylate) than for rigid polysaccharides (e.g., galactomannans) although the complexation mechanism is very similar.

Registry No. 1,2-Propanediol, 57-55-6; borax, 1303-96-4; poly(glyceryl methacrylate), 28474-30-8; poly(vinyl alcohol), 9002-89-5; galactomannan, 11078-30-1.

References and Notes

(1) Tsuchida, E.; Nishide, H. *Adv. Polym. Sci.* 1977, *24*, 1.
(2) Menjivar, J. In *Water Soluble Polymers*; Glass, L., Ed.; American Chemical Society: Washington, DC, 1986, p 809.
(3) Allain, C.; Salome, L. *Macromolecules* 1987, *20*, 11, 2957.
(4) Pezron, E.; Liebler, L.; Ricard A.; Audebert, R. *Macromolecules* 1988, *21*, 1126.
(5) Ochiai, H.; Kurita, Y.; Murakami, I. *Makromol. Chem.* 1984, *185*, 167.
(6) Ochiai, H.; Shimizu, S.; Tadokoro, Y.; Murakami, I. *Polym. Commun.* 1981, *22*, 1456.
(7) Tsuchida, E.; Nishikawa, H. *J. Phys. Chem.* 1975, *79*, 2072.
(8) Leibler, L.; Pezron, E.; Pincus, P. *Polymer* 1988, *29*, 1105.
(9) Pezron, E.; Leibler, L.; Lafuma, F. *Macromolecules*, submitted.
(10) Roy, G. L.; La Ferriere, A. L.; Edwards, J. D. *J. Inorg. Nucl. Chem.* 1957, *4*, 106.
(11) Henderson, W. G.; How, M. J.; Kennedy, G. R.; Money, E. F. *Carbohydr. Res.* 1973, *28*, 1.
(12) Van Duin, M.; Peters, J. A.; Kieboom, A. P. G.; Van Bekkum, H. *Tetrahedraon* 1985, *41*, 3411; 1984, *15*, 2901.
(13) Sinton, S. W. *Macromolecules* 1987, *20*, 2430.
(14) Shibayama, M.; Sato, M.; Kimura, Y.; Fujiwara, H.; Nomura, S. *Polymer* 1988, *29*, 336.
(15) Gey, G.; Noble, O.; Perez, S.; Taravel, F. R. *Carbohydr. Res.* 1987.
(16) Pezron, E.; Ricard, A.; Lafuma, F.; Audebert, R. *Macromolecules* 1988, *21*, 1121.
(17) Refojo, M. F. *J. Appl. Polym. Sci.* 1965, *9*, 3161.
(18) Macret, M.; Hild, G. *Polymer* 1982, *23*, 81.
(19) Morawetz, H. *J. Polym. Sci.* 1957, *23*, 247.
(20) de Gennes, P.-G. *Scaling Concept in Polymer Physics*; Cornell University Press: Ithaca, New York, 1979.
(21) Des Cloizeaux, J. *J. Phys. (Paris)* 1980, *401*, 223.
(22) Cates, M. E.; Witten, T. A. *Macromolecules* 1986, *19*, 732.

Kinetics and Mechanisms for Thermal Imidization of a Polyamic Acid Studied by Ultraviolet–Visible Spectroscopy

Eumi Pyun, Richard J. Mathisen, and Chong Sook Paik Sung*

Institute of Materials Science, Department of Chemistry, 97 North Eagleville Road, University of Connecticut, Storrs, Connecticut 06268. Received April 20, 1988; Revised Manuscript Received August 22, 1988

ABSTRACT: The kinetics and the mechanisms of thermal imidization of polyamic acid made from a conjugated diamine (p,p'-diaminoazobenzene) and a nonconjugated dianhydride (6F-DA) were investigated both in dilute solution and in solid state in the temperature range 150–190 °C. UV–vis absorption spectroscopy was the main tool used even though IR spectroscopy was also used for comparison with the results from UV–vis studies. UV–vis spectral changes as a function of imidization time were analyzed on the basis of the previously reported model compound studies in order to obtain the composition of various imidization species (*Macromolecules* 1987, *20*, 1414). In 1% *N*-methylpyrrolidone solution, dissociation and the first imide ring closure proceed faster than the second imide ring closure of polyamic acid/imide at all three temperatures studied (150, 170, and 190 °C). This trend is attributed to the reduced basicity of the amide group in polyamic acid/imide in comparison to the analogous group in polyamic acid. Activation energies for the fast process and the second ring closure were 11 and 18 kcal/mol, respectively. During the early stages of imidization in dilute solution, IR spectra suggest some dissociation of polyamic acid as well as imidization. On the basis of these findings, the mechanism of imidization for dilute solution has been proposed. In solid-state imidization, the apparent imidization rate was initially faster than in dilute solution due to the catalytic effect of the neighboring amic acid group but levels off probably due to vitrification. Therefore, the mechanism of solid-state imidization must take into account the catalytic effect of the neighboring amic acid groups and the decreasing mobility effect as a function of cure time. Modeling studies to predict spectral changes as a function of the ratio of the two imidization rate constants are consistent with the observed results in dilute solutions. The results are adequately modeled by assuming a first-order, two-step imidization reaction, assuming a small extent of dissociation. On the other hand, solid film results seem to be reasonably simulated by assuming a second-order reaction for the first step, followed by a first-order reaction for the second step to account for the decrease in the concentration of the conformationally favorable catalytic amic acid group. Finally, there is a good correlation between UV–vis results and IR results, in regard to the overall extent of reaction in solid films.

Introduction

Polyimides are an important class of high-performance polymers. Excellent mechanical and electrical properties as well as high-temperature stability make these polymers suitable for applications in the aerospace industry as high-performance composites and in the electronics industry as high-temperature coatings. Difficulty in processing, however, has slowed the widespread use of these

Scheme I
Simplified Two-Stage Reaction Scheme for the Polyimide Synthesis

polyamic acid

polyimide; R = aromatic group

Scheme II
Polyimide Reaction Scheme

R = conjugated aromatic group
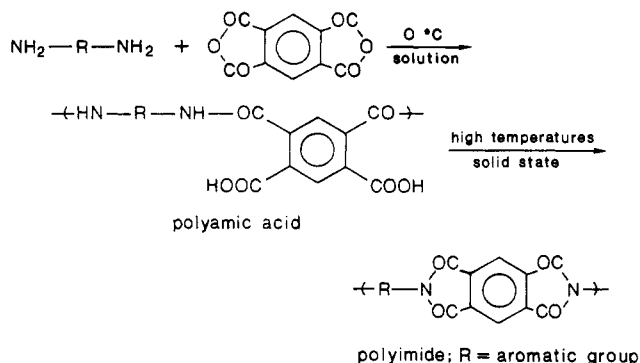
polymers by making them expensive and limiting their applicability. Factors responsible for this problem include poor solubility and the evolution of volatiles during heat treatment.[1] The presence of voids in thick films is common because of residual solvent and byproduct volatilization throughout processing. Another reason for processing problems is the lack of information about the imidization mechanisms and kinetics; previous studies of these processes, especially solution studies, have often been contradictory and incomplete.[2] In industry, complex, empirically established, and costly multistage processing is often employed to reduce these problems.

In order to shed light on the kinetic parameters and the mechanisms involved in thermal imidization, we explored electronic spectroscopy as a characterization tool. By utilizing UV–vis absorption spectra, we were recently able to distinguish several imidization products as demonstrated with the model compounds and to quantify their formation and disappearance.[3] Such a distinction has not yet been possible by other spectroscopic techniques such as IR or NMR.

Before elaborating on this technique, it is important to review the chemistry of polyimides and the results of the imidization studies by other spectroscopic characterization techniques. In the following section, we also propose a new reaction scheme (Scheme II), including a two-step imidization process applicable in some cases.

Polyimide Synthesis: Reaction Schemes. Linear polyimides are made by the imidization of polyamic acids, which are formed by the reaction of dianhydride with diamine. While polyamic acid formation proceeds quickly at low temperatures, imidization requires much higher temperatures. These two stages are usually considered separately as illustrated in Scheme I. Polyimides can be classified into four groups, depending on whether the diamine or the dianhydride is conjugated or not. Each of these groups has different final properties as well as different processing requirements.[1b] The reason for this trend can be understood in view of the nature of the reactions involved.

The formation of polyamic acids from diamines and dianhydrides proceeds via nucleophilic substitution on the anhydride carbonyl atom with the amine acting as a nucleophile. It has been shown that the reaction rate is dependent on the basicity of the amine, the electrophilicity of the anhydride carbonyl, and the basicity of the solvent.[4a] It is well-known that the formation of polyamic acids is a reversible reaction where the factors described above play important roles in determining the rate constants and the equilibrium constants.[4b] This reversible degradation of polyamic acids into amines, acids, or anhydrides constitutes a serious competing reaction with the imidization
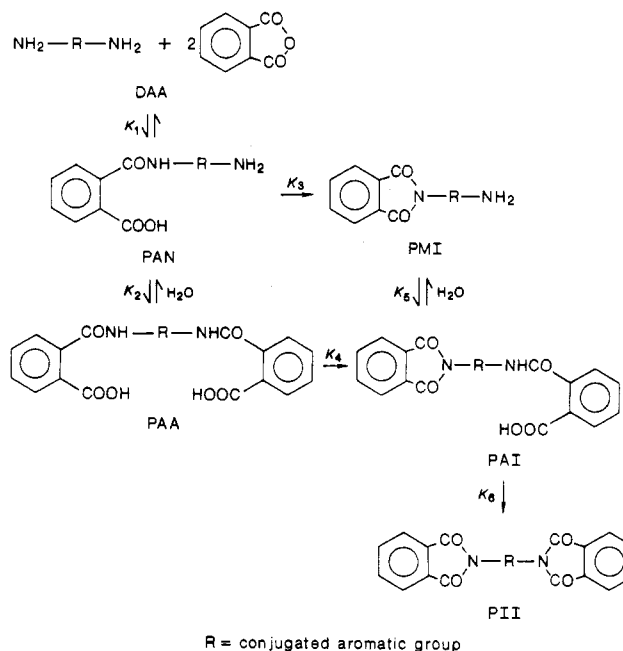
step, as illustrated in Scheme II.[1a,b]

The thermal imidization of polyamic acids involves cyclization through the nucleophilic attack on the acid carbonyl carbon by the free electron pair of the amide nitrogen. As is the case in the formation of polyamic acids, imidization kinetics are complicated by many factors including the properties of the solvent and the precursor polyamic acids. Reaction rates have been found to increase with decreasing solvent basicity in both solid films[5a] and solutions.[2c]

Lavrov and co-workers showed that the cyclization rate is accelerated by an increase in the electron density on the amide nitrogen, which is directly related to the basicity of the initial amine.[2b] They also suggested that the reactivity would further increase with the electrophilicity of the acid carbonyl. In addition to the reversible hydrolysis of the amide group from polyamic acids (PAA), another hydrolytic reaction can occur from polyamic acid/imide (PAI) to a reacted species (PMI) containing imide and amine as illustrated in Scheme II. Nonconjugated diamines or dianhydrides have spacer groups such as carbonyl, oxygen, or sulfur between aromatic rings. These groups inherently influence the basicity of the amines or the electrophilicity of the anhydride carbonyl mainly by inductive effects, so that their reaction rates are different from those of conjugated systems. However, the reactivity of amine, anhydride, or amic acid at the para position in the conjugated system is expected to be strongly influenced by the substituent at the para' position. This is because a strong electron acceptor such as an imide group para to the amide nitrogen is found to increase the extent of hydrolysis dramatically.[6]

For example, in the case of the conjugated diamine, the hydrolysis step characterized by the equilibrium constant k_5 is probably more important than the hydrolysis step from PAA characterized by k_2. In Scheme II, we also chose to write the cyclic imidization by a two-step process (k_4 and k_6). This scheme proposes the formation of an alternating amide–imide backbone prior to complete imidization. This idea is justified in the case of the conjugated diamine since the reactivity of the amide nitrogen in PAI in comparison to PAA is expected to be lower due to the electron-withdrawing imide group in PAI. Indeed, Lavrov

et al. confirmed that the electron-accepting or -withdrawing nature of the substituent para to the amide nitrogen is the single largest factor in determining the imidization rate of model mono amic acids.[2b] To the best of our knowledge, such a two-step imidization process has never been experimentally observed. This is due to the fact that IR spectroscopy, which is most often used to follow the kinetics of imidization, cannot distinguish between the two major imide species (PAI and PII).

Imidization kinetics are also influenced by factors such as solvent content and the physical state of the polyamic acid. Brekner and Feger reported that the hydrogen-bonded complex formed between the solvent *N*-methylpyrrolidone (NMP) and polyamic acids can prevent the reactive groups of the amic acid from getting into the conformation required for imidization to occur.[7] They noted that this effect is less pronounced in solution than in the solid state because the constant solvent exchange in solution increases the conformational mobility of the reactive groups. Ginsburg and Susko demonstrated that the rate of reaction in solid films increases with film thickness due to solvent retention.[8] Polyamic acids have generally lower T_gs than polyimides. Therefore, during the solid-state reaction of polyamic acids, vitrification can occur due to the solvent loss as well as the imidization.[9] It is speculated that the evaporation of solvent and water (an imidization byproduct) as well as the imidization itself is controlled by vitrification.

All the factors discussed above such as the types of monomers and residual solvents, the competing reactions, and the physical state of the reaction strongly influence the imidization characteristics of polyamic acids. The limited solubility of polyimides further adds to the difficulty of their characterization, and consequently most studies of them have been limited to solid-state reaction studies by IR spectroscopy.[8,10] In solutions such as *N*-methylpyrrolidone, solvent interference in IR spectra usually renders quantitative analyses difficult at best. Some researchers have tried to minimize this by precipitating polyimides in water before IR analysis, but this process could introduce errors due to the competing hydrolysis of the unreacted amide groups.[10b]

Review of IR and NMR Studies. As mentioned above, the most widely used technique for monitoring polyimide formation is infrared spectroscopy. Absorption bands characteristic of the imide ring occur at 1770–1800 cm^{-1} due to the symmetric imide carbonyl stretch, at 1370–1380 cm^{-1} from the imide carbon–nitrogen stretch, and near 721 cm^{-1} due to the imide ring bending. The latter two absorptions can be used for quantitative studies, but the carbonyl absorption may deviate from the Beer–Lambert law due to hydrogen bonding.[2a] The extent of imidization by IR spectroscopy is usually estimated by a ratio of the imide peak with a reference aromatic vibration. The common trend observed in such plots of imidization extent versus time in the solid films is a rapid initial rate followed by a more gradual conversion.

Several ideas have been proposed to account for the apparent two-step cyclization, including the nonequivalent kinetic states of the amic acid groups,[11] vitrification as defined before, or the decomposition of polyamic acids back to the anhydride and amine groups. However, it is not possible to decide which if any of these idea(s) is responsible for the kinetic behavior since the IR method only provides overall imide ring concentration and thus cannot differentiate between different reacted such as PII, PAI, and PMI in Scheme II. Very recently, nitrogen-15 NMR using dipolar decoupling, cross polarization, and magic

Scheme III
Chemical Structures of the Diamine and Dianhydride Used in This Study
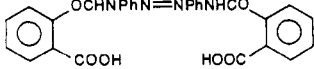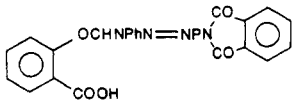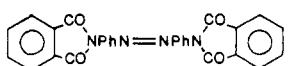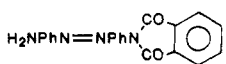

diaminoazobenzene (DAA)

6F–DA
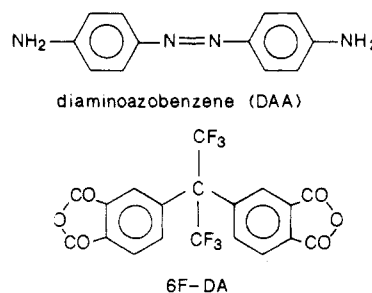
angle spinning has been explored to characterize the reaction to polyimides.[12] Weber and Murphy were able to identify imide, amide, and amine peaks in enriched N-15 NMR spectra.[15] However, quantitative analyses are not yet available since the detailed knowledge of the relaxation parameters for each type of nitrogen is needed and it has not yet been demonstrated whether N-15 NMR can distinguish between different reacted species such as PAI and PII.

Design of the Experiments. In order to thoroughly understand and optimize the imidization process both in solution and in the solid state, we needed a technique to differentiate between the various reacted species shown in Scheme II, one which would not be influenced by the presence of the solvent. For these requirements, we chose UV–visible absorption spectroscopy because a solvent such as NMP does not interfere with the polymer absorption in most of the UV–visible range. If the various reacted species show sensitive changes in fluorescence, that can also be used. Unfortunately, the cyclization species studied in this work did not exhibit much fluorescence. As for the polyimide system, we chose a conjugated diamine and a nonconjugated dianhydride in order to reduce the charge-transfer complex formation known to occur when both monomers are conjugated.[13,14] The charge-transfer complexes are usually intensely colored and could interfere in the UV–vis spectra. In this study, diaminoazobenzene (DAA) is used as a conjugated diamine, while a fluorinated dianhydride is used as a nonconjugated dianhydride (see Scheme III for their chemical structures.) Recently, we have used DAA to study the cure reactions and species with diepoxide.[15] In epoxy systems, we took advantage of the magnified spectral shifts when the two amino substituents are at the opposite para positions. As the diamino groups are chemically transformed to the secondary and the tertiary amines, the bathochromic spectral shifts and the large enhancement of the fluorescence intensity were observed in UV–vis absorption spectra and fluorescence spectra, respectively. By analyzing these spectral changes, we were able to monitor composition, the kinetic parameters, activation energy, and extent of reaction.

In polyimides, UV–vis spectral shifts as well as the changes in the extinction coefficients are also observed, depending on the reacted species.[3] This is observed when using DAA as the diamine because of the unique electronic states associated with each cure species. As we recently demonstrated, the diamic acid derivative of DAA shows a blue shift of 20 nm from that of DAA. This shift is due to the weaker electron-donating capacity of the amide bond as compared to the amine toward the conjugated azo bond. When one of the amic acids is cyclized, a red-shift of about 20 nm results from the greater resonance induced by the push–pull effect of the amide–imide combination. Imidization at both sides of diamic acids destroys this effect and greatly reduces the electron density near the azo

<p style="text-align:center">Table I
Absorption Maxima, Spectral Shifts, and Extinction
Coefficients of Various Imidization Products of
Diaminoazobenzene (DAA)</p>

compound	λ_{max}, nm	$\Delta\lambda$,[a] nm	$\epsilon \times 10^{-4}$, L/mol·cm
H₂NPhN=NPhNH₂ DAA	415	0	4.5
diamic acid	393	−22	3.9
amic acid-imide	413	+20	2.0
diimide	343	−68	3.0
amine-imide	417	+4	3.1

[a] This is the successive spectral shift. For diimide and amine–imide, the spectral shift is measured from amic acid–imide, as illustrated in the sequence of reactions in Scheme II.

linkage. Thus, a large blue shift is observed for the diimide derivative of DAA. For amine–imide, which can be a hydrolysis product from amic acid–imide, the absorption maximum appears at 417 nm, due to the push–pull effect. Since the amine is more donating than the amide, the absorption maximum occurs at a slightly longer wavelength than that of the amide–imide species. Table I summarizes the absorption maxima, spectral shifts, and extinction coefficients of various DAA derivatives expected from the imidization process. Scheme IV shows the reaction routes used for the syntheses of various model reacted species.[3]

Experimental Section

Materials. Diaminoazobenzene (DAA) was purchased from Eastman Kodak and recrystallized from methanol. Electronic grade dianhydride, 6F-DA, 5,5′-[2,2,2-trifluoro-1-(trifluoromethyl)ethylidene]bis(1,3-isobenzofurandione), was a gift with American Hoechst and used without further purification. *N*-methylpyrrolidone (NMP) was purchased from Aldrich, dried over molecular sieve type 4A, and distilled twice at reduced pressures. Freshly distilled NMP was used for imidization studies.

Imidization Studies. NMP complicates imidization studies in solid films due to its complex formation with polyamic acid[7] and its high boiling point, which makes it difficult to remove; so we used acetone as the casting solvent. All glassware used for polyamic acid and polyimide synthesis was oven dried at 100 °C for 1 h. Equal moles of DAA (0.0808 g) and 6F-DA (0.1962 g) were each dissolved in 1.5 mL of acetone and cooled to 0 °C. The dianhydride solution was slowly added to the diamine solution and the well-mixed solution was kept at 0 °C for 30 min to make polyamic acids. A thin polyamic acid film was cast on a large Petri dish and vacuum dried for 2 days to remove the acetone. After removing the acetone, we obtained films of polyamic acids which are about 1 mil in thickness. IR spectra of these films confirmed the presence of amic acid structure by characteristic absorptions at 3280 (NH), 3100 (OH), 1669 (C=O), 1598 (C=O), and 1537 (NH) wavenumbers. Only trace amounts of unreacted anhydride were detected in the IR spectra. The UV–vis spectra in NMP solution showed the main absorption peak at 393 nm, corresponding to the diamic acid absorption. In addition, significant absorption at 415 nm due to the presence of imide–amide species was also observed. IR spectra confirmed the presence of some

<p style="text-align:center">Scheme IV
Reaction Scheme for the Synthesis of Model Imidization
Products of Diaminoazobenzene</p>
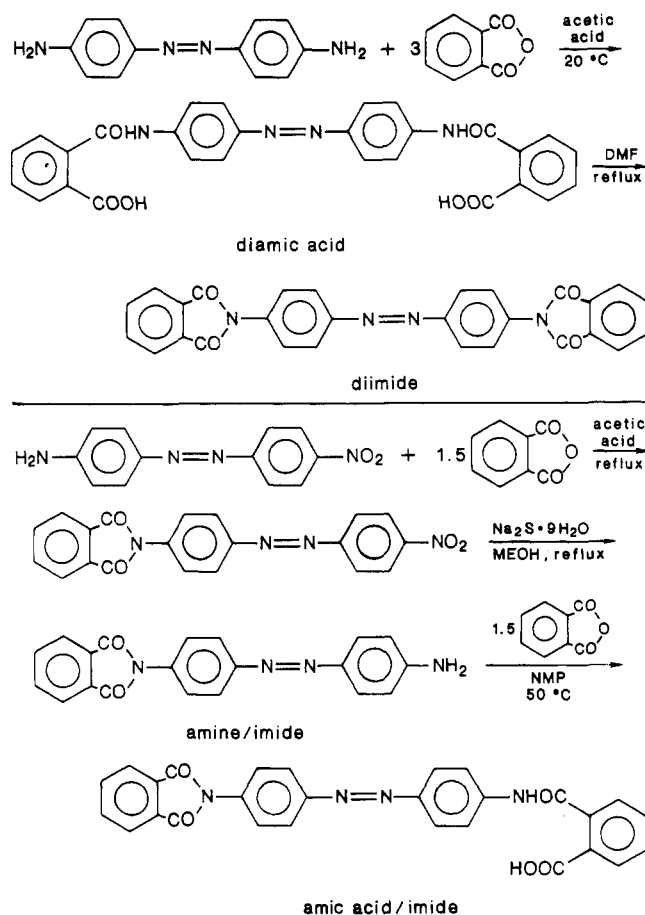
imide peaks. Therefore, the polyamic acid films we used for imidization studies were not 100% polyamic acid, but rather partially imidized or dissociated polyamic acids. Attempts to synthesize 100% pure polyamic acids were not successful.

The thermal imidization of these partially imidized or dissociated polyamic acid films was followed by the shifts in the UV–vis spectra at various temperatures and concentrations. Sroog and co-workers noted the poor hydrolytic stability of polyimides derived from conjugated diamines.[6] Since our system employs a conjugated diamine, particular care was taken to facilitate the removal of water formed during imidization. The requirement of constant concentration complicates the removal of water because of possible solvent loss. In order to overcome these problems, the reaction apparatus using a three-necked flask was set up where a Dean Stark tube was used in the center neck instead of a condenser so that water vapor could exit the reaction flask without loss of solvent. A constant flow of dried argon as purge gas was maintained so that water vapors were carried out of the reaction at a constant rate. Films were dissolved in freshly distilled NMP to the desired concentration and well-stirred solutions were purged with dried argon before immersion in the preheated constant-temperature bath. Samples of 5 μL in volume were taken out of the reaction flask through the rubber septum by using a microsyringe. Samples were diluted to a constant concentration (1.33 × 10⁻⁵ g/L) in freshly distilled NMP before spectra were taken.

As with solution studies, the reaction conditions in solid film imidizations are most important. We used a modified, round-bottomed flask with a long, tapered side arm. Small pieces of the polyamic acid film were placed into the lower bulb and the reaction apparatus was purged with dried argon before being immersed in the preheated, constant-temperature bath. Samples were taken out with a long spatula at set time intervals and dissolved in NMP for spectral analysis. The purge gas inlet tube was extended well into the oil bath before it entered the reaction flask, allowing the gas to be heated before entering the reaction

chamber and the water vapor formed during imidization to be pushed out. The flow rate of purge gas was kept constant. Since the weights of the film pieces were not always the same, the polymer concentration after dissolving in NMP was not constant for solid film studies.

Spectroscopic Characterization. Infrared spectra were recorded on a Nicolet 60SX FT-IR spectrophotometer. UV–vis spectra were recorded on a Perkin-Elmer Lamda Array spectrophotometer (Model 3840 with a 7600 Data Station).

Results and Discussion

Modeling Spectral Changes Based on Imidization Kinetics. Before we quantitatively analyzed UV–vis spectral changes in terms of imidization kinetics, we carried out some modeling studies to predict how the kinetic parameters could influence the spectral changes. It is important to realize that we always observed red shifts in epoxy curing as the DAA label was converted to the secondary and tertiary amines. However, in imidization, the first imide ring closure (PAI in Scheme II) results in a moderate red shift (~ 20 nm) while the second imide ring closure (PII in Scheme II) is followed by a greater blue shift (~ 70 nm). In this case, the magnitude of the ratio of the two imidization rate constants, k_1 and k_2 as defined below, is found to determine the overall spectral changes.

From Scheme II, we can write the following three kinetic differential equations for the two main imidization reactions by neglecting other competing reactions.

$$\underset{X}{PAA} \xrightarrow{k_1} \underset{Y}{PAI} \xrightarrow{k_2} \underset{Z}{PII}$$

$$-dx/dt = 2k_1x \tag{1}$$
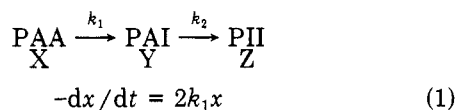
$$-dy/dt = -2k_1x + k_2y \tag{2}$$

$$dz/dt = k_2y \tag{3}$$

where x, y, and z are the fraction of PAA, PAI, and PII, respectively, and their sum is equal to unity.

Equations 2 and 3 can be solved in terms of x assuming that r is equal to $k_2/2k_1$ as shown in eq 4 and 5. On the

$$y = -x/(1 - r) + x^r/(1 - r) \tag{4}$$

$$z = 1 + (r/(1 - r))(x/r - x) \tag{5}$$

basis of eq 4 and 5, one can calculate y and z values for a series of x values given the ratio r. Figure 1 illustrates plots of x, y, and z values for two different r values as a function of the extent of overall imidization, ξ_i, which is defined by eq 6.

$$\xi_i = (y + 2z)/2 \tag{6}$$

As expected, Figure 1 shows that the formation of diimide species (z) occurs sooner when k_2 is the same as k_1 ($r = 0.5$) as compared to the case when k_2 is much smaller than k_1 ($r = 0.05$).

Now, the next step is to generate UV–vis absorption spectra for a wide range of r values by digital addition corresponding to sets of x, y, and z values from the stored spectra of each species. Examination of a series of the spectra thus generated shows that the overall spectral response can be divided into two trends depending on the magnitude of r. When R is greater than 0.3 no red shift is predicted before blue shifts occur, as illustrated in the top spectrum of Figure 2 for the case of r being equal to 0.5. When r is less than 0.3, some red shift is first predicted, followed by the blue shifts. However, when r is less than 0.001, a maximum red shift of 24 nm, from 345 to 415 nm, is predicted as shown in the lower spectra of Figure 2 for the case of $r = 0.0001$. This amount is the maximum possible value since λ_{max} of PAI is at 415 nm. For the r
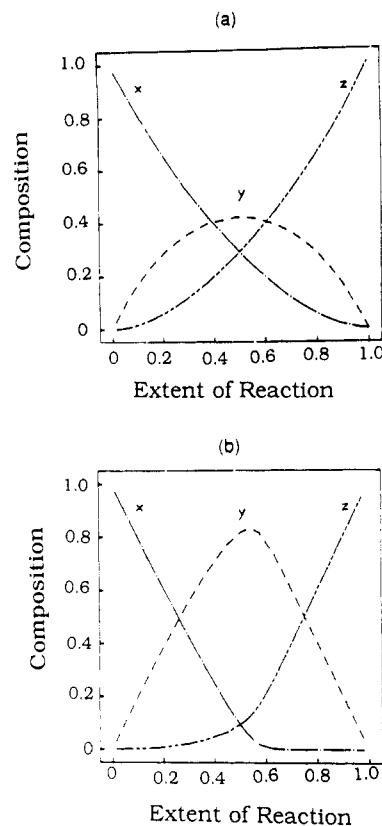

Figure 1. Theoretical prediction of the composition of the imidization species as a function of overall extent of reaction (ξ) according to eq 4–6 for two different reactivity ratios [(a) for $r = 0.5$; (b) for $r = 0.05$].

values between 0.001 and 0.3, the amount of the initial red shift predicted initially is smaller than the maximum. In fact, it is a strong function of r as illustrated in Figure 3, varying from zero to 24 nm.

The trends predicted by this type of modeling are useful in understanding the actual experimental data, when dissociation can be assumed to occur to a small extent.

Imidization Studies in NMP Solution. 1% Polyamic Acid in NMP Solution. The isothermal imidization of polyamic acids in 1% (by weight) NMP solution was followed by UV–vis spectroscopy at three temperatures (150, 170, and 190 °C). Samples were taken out of the reaction flask at various times and diluted to a set concentration before spectra were taken. Figure 4 shows a series of UV–vis spectra as a function of reaction time at 150 °C. Figure 4 is distinguished by two stages. At the early reaction times (Figure 4a), the absorption peaks are first red-shifted to longer wavelengths, due to either the formation of amic acid/imide species (PAI in Scheme II) and/or the dissociation products (DAA or PAN in Scheme II). At 150 °C, it takes only about 40 min for the red shifts to be completed. After that, the spectra is hardly shifted until the cure time of about 180 min, but there is a decrease in absorbance. During this time interval, the diimide formation is at best very small as judged by the small absorbance at 343 nm. In the longer reaction times (Figure 4b), the diimide (PII species in Scheme II) is formed as indicated by the growing peak at 343 nm and the decreasing peak at 413 nm. The 170 and 190 °C reaction exhibited spectral features very similar to the 150 °C reaction. The presence of the isosbestic point in the second stage of the reaction indicates that only two reaction intermediates, PAI and PII species, are present.

The absence of the isosbestic point in the first stage of the experimental data (Figure 4a) seems to support that
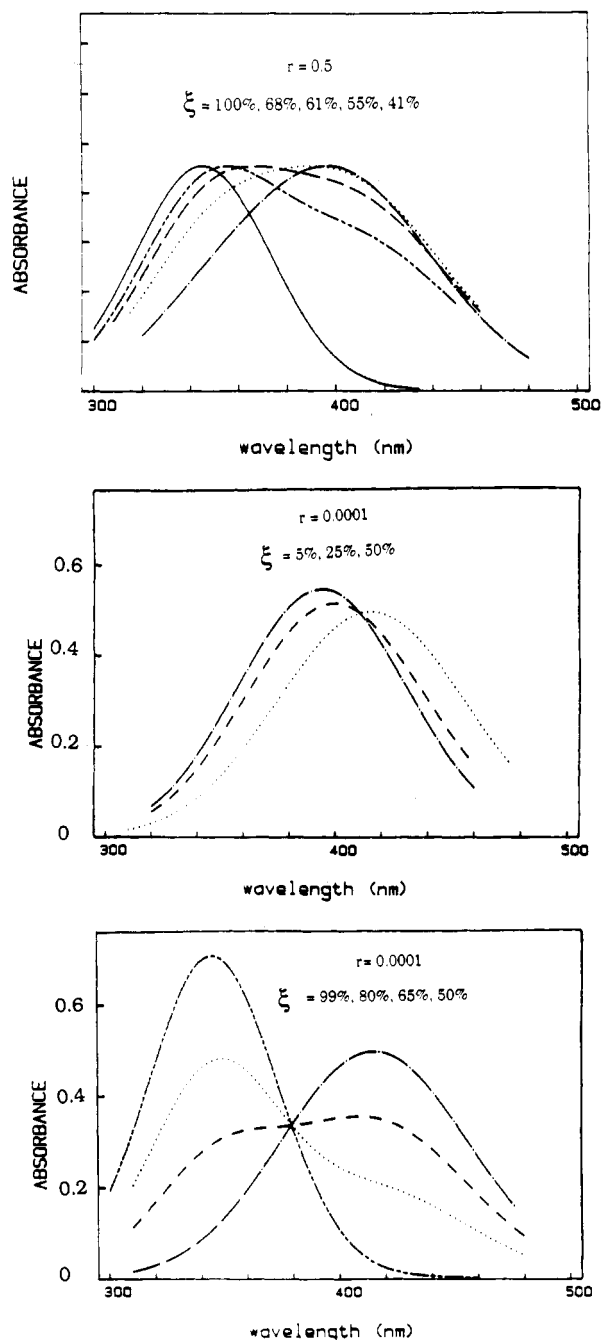
Figure 2. Theoretically generated UV–vis spectra for different reactivity ratios as a function of overall extent of reaction [(top) for $r = 0.5$; (bottom two spectra) for $r = 0.0001$].

the conversion of polyamic acid/imide (PAI) is not the only reaction in the first stage and that there are probably some dissociation products being formed by competing side reactions. Two possible side reactions are shown in Scheme II: the hydrolysis of PAA to PAN (polyamic acid/amine) and the hydrolysis of PAI to PMI (polyamine/imide). Preliminary FTIR studies confirm that imidization indeed occurs in 1% NMP solution of polyamic acids, but not as fast as UV–vis studies indicate when no dissociation is assumed. However, the extent of imidization by IR measured at 721 cm^{-1} is greater than the results by UV–vis studies when complete dissociation is assumed in the first stage. Together with the appearance of free amine absorption bands in IR spectra, the IR results, in comparison to UV–vis results, can be interpreted as suggesting some dissociation as well as the formation of the amic acid/imide species during the first stage. Unfortu-
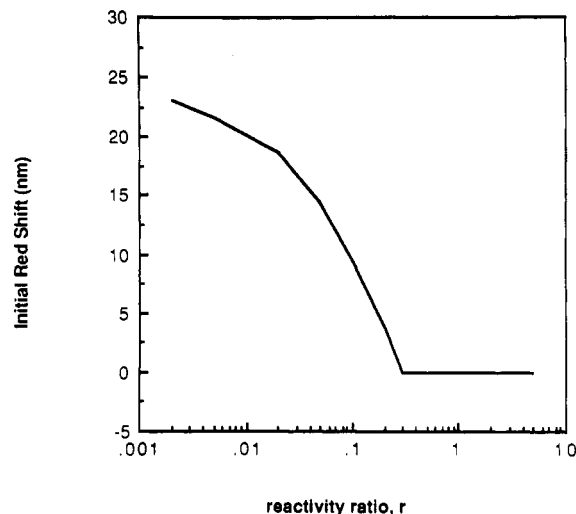

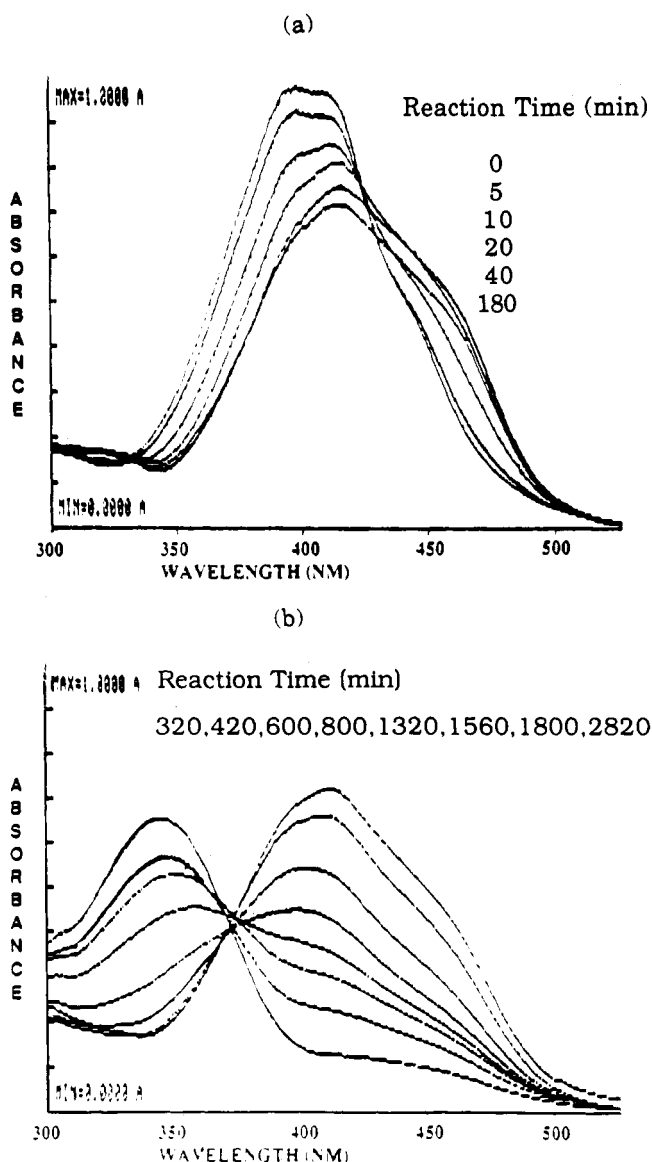**Figure 3.** Extent of the initial red shift predicted as a function of the reactivity ratio, r.

(a)

(b)

Figure 4. UV–vis spectra following imidization of polyamic acid based on 1% DAA and 6F-DA in NMP solution at 150 °C [(a) for early stages of reaction; (b) for later stages of reaction].

nately, it is difficult to quantify how much dissociation occurs. Therefore, we propose Scheme V as a representative reaction pathway occurring in 1% solution reaction.

Scheme V
Proposed Reaction Pathways for Imidization of 1%
Polyamic Acid in NMP Solution

first stage :

$$PAA \xrightarrow{K_1} PAI$$

$$\downarrow$$

$$PAN$$
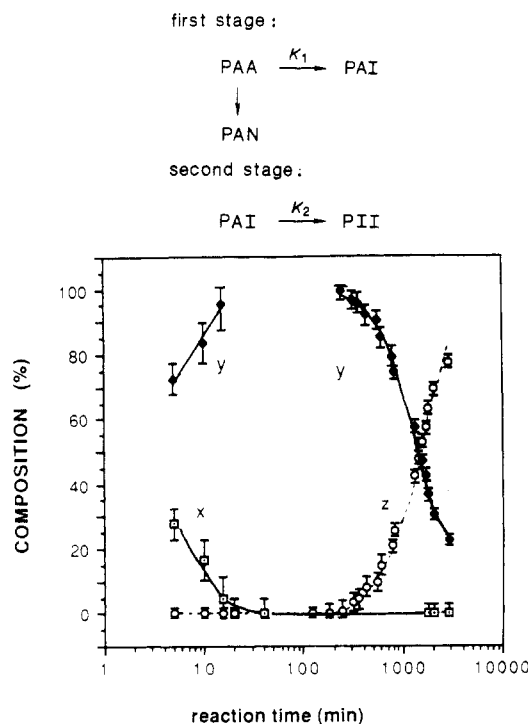
second stage :

$$PAI \xrightarrow{K_2} PII$$

Figure 5. Experimental composition of imidization species as a function of reaction time at 150 °C for 1% polyamic acid in NMP solution. (The maximum deconvolution error is ±8%.)

Now we can attempt to obtain more quantitative data to characterize the rate constants involved in the reaction pathways shown in Scheme V. Quantitative analyses require the deconvolution of the spectra to obtain the composition of the species. In the second stage of imidization, we are justified in assuming only two species, PAI and PII. The first stage and the intermediate period during which the spectra only show changes in intensity are more difficult to treat in a quantitative way. Therefore, we analyze the first few data points in the first stage by assuming that only PAA and PAI are involved and that dissociation occurs only to a small extent.

Figure 5 illustrates an example of the composition of the three main reacted species at 150 °C by the deconvolution of the UV–vis spectra based on the above assumptions. The PAI is formed quickly with subsequent decrease of PAA. Since there is some dissociation going on during the first stage, the concentration of PAI represents the maximum possible value. Between 40 minutes to 180 minutes, we speculate some conversion of PMI to PAI, as deduced from the decrease in spectral intensity. Therefore, it is difficult to estimate the concentration of PAI in this time period, even though it is certain that there is no significant concentration of the diimide (PII) species present. After 180 min of imidization, the spectra can be easily deconvoluted with only two cure species, PAI and PII. As shown in Figure 5, PII is slowly formed following decrease of PAI. After 2820 min, the PII fraction is about 78% while the PAI fraction is 22%. This corresponds to the overall imidization extent of 89%. The maximum deconvolution error in the composition of the reacted species could be ±2% to ±7% as shown in Figure 5. At 170 and 190 °C, the general features of the reacted composition are exactly the same as in Figure 5, except that the reactions are faster and reach higher conversion.

In order to obtain more quantitative rate constants and *r* values from the experimental data, we use the following
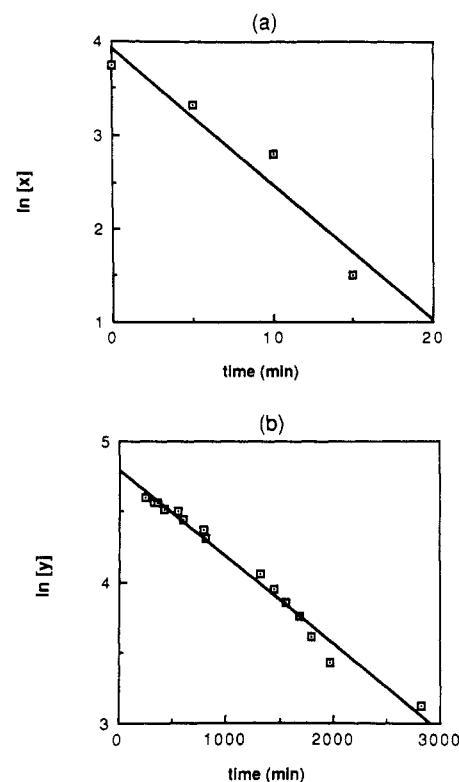

Figure 6. First-order kinetic plot of ln *x* or ln *y* versus reaction time for imidization at 150 °C of 1% amic acid in NMP solution [(a) for ln *x* versus time plot; (b) for ln *y* versus time plot].

Table II
Imidization Rate Constants, k_1 and k_2, and the Activation Energies for Reaction of 1% Polyamic Acid in NMP

T, °C	$2k_1$, min⁻¹	$E_a = 11$ kcal/mol; ln $A = 11$ min⁻¹	$10^3 k_2$, min⁻¹	$E_a = 18$ kcal/mol; ln $A = 13$ min⁻¹	$10^3 r$
150	0.145		0.62		4.28
170	0.171		1.40		8.19
190	0.465		3.80		8.17

solutions for the kinetic equations for the proposed reaction pathway (Scheme V).

$$\ln x = -2k_1 t + \text{constant} \tag{7}$$

$$\ln y = -k_2 t + \text{constant} \tag{8}$$

where *x* and *y* are the fraction of PAA and PAI, respectively. Equation 7 is an approximate solution for the initial stage of the imidization reaction where the dissociation is considered to be small. Figure 6a and (b) illustrates the plots of ln *x* or ln *y* as a function of time at 150 °C cure. It is noted in Figure 6a that k_1 is based on only four data points while k_2 is based on many more data points. Similar analyses were carried out for the data at 170 °C and 190 °C. Parts a and b of Figure 7 show Arrhenius plots for k_1 and k_2, respectively. Table II summarizes the values of k_1, k_2, and *r* as well as the activation energy for each step. As seen from the last column of Table II, *r* is less than 0.01 at all three imidization temperatures, indicating a much faster rate of the first process. The activation energy for the first process is about 11 kcal/mol while the analogous energy for the second imide ring closure is about 18 kcal/mol. The preexponential factors for the two processes are similar as shown in Table II. The activation energy values observed in this study compare favorably with the value observed for the initial stage imidization of pyromellitic dianhydride with aniline in dilute solution (16) as well as that of imidization of a polyamic acid.[17] A wide range of the preexponential factors had also been reported,
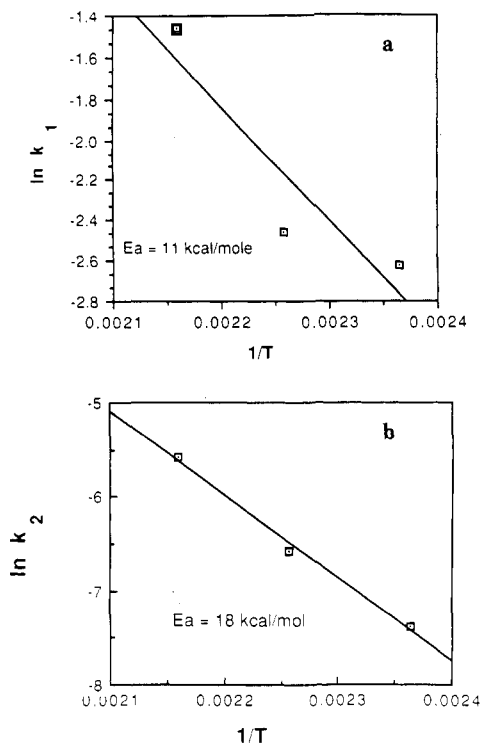
Figure 7. Arrhenius plot of ln k_1 or ln k_2 versus $1/T$ [(a) for ln k_1; (b) for ln k_2].
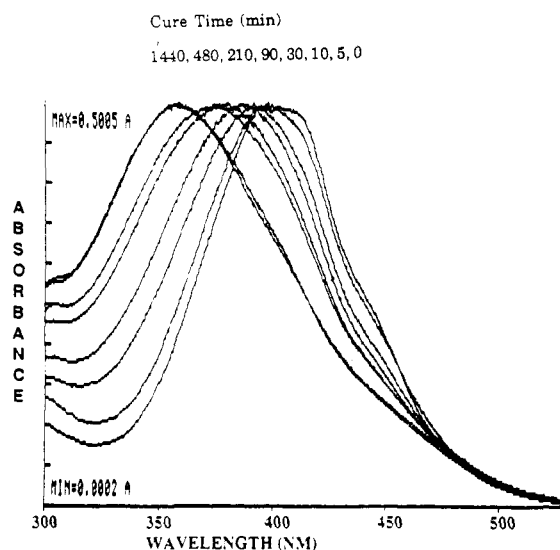

Figure 8. UV–vis spectra following imidization of polyamic acid film based on DAA and 6F-DA at 150 °C in solid state.

depending on the chemical structures and the state of the samples.[16,17]

Imidization Studies in Solid State. The isothermal imidization of partially imidized polyamic acid films was monitored by UV–visible spectroscopy at three temperatures (150, 170, and 190 °C). It is known that the basicity of the solvent affects the imidization processes[2c,5a] and also that NMP forms complexes with polyamic acids.[7] Furthermore, the decomplexation kinetics is known to be quite temperature and time dependent. In order to avoid these potential complications, we chose acetone as a solvent and, prior to the imidization studies, we removed it completely.

Figure 8 shows a series of UV–visible spectra as a function of reaction time at 150 °C where blue shifts are observed. Also, at other temperatures (170 and 190 °C), only blue shifts occur, but with much faster rates of change. In view of the modeling studies to predict spectral changes as described in the preceding section, blue shifts without
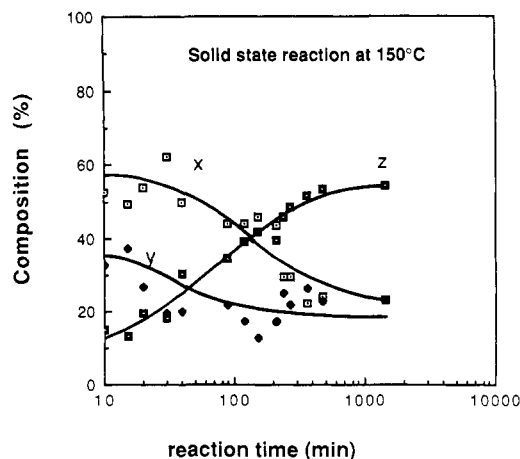

Figure 9. Experimental composition of imidization species as a function of reaction time at 150 °C in the solid state. (The maximum deconvolution error is ± 10%.)

the initial red shifts are predicted when r is greater than 0.3 if we assume the same first-order kinetics. This corresponds to a k_1 less than 1.6 times k_2, whereas in dilute solution, k_1 is observed to be much faster compared to k_2. This trend was explained due to the electron-withdrawing effect of the imide group para to the amic acid in poly(amic acid–imide). As a result, the reactivity of the amic acid in polyamic acid is predicted to be larger than that of the amic acid/imide. This is believed only to be true in dilute solutions since the addition of carboxylic acids is known to catalyze the imidization.[2c] In fact, up to a certain concentration of acids, a linear relationship between the rate constants and the acid concentration has been observed. When the concentration of the solution begins to increase to the extent that the chains of polyamic acids overlap, then the amic acid groups in the neighboring chain can catalyze the imidization intermolecularly. In fact, our experiments seem to support this argument. When we studied imidization in a 7.5 wt % solution, we observed a red shift, followed by a blue shift. However, the magnitude of the red shift was only about 16 nm. According to Figure 3, such a magnitude is predicted when the r value is about six times greater than that in a dilute (1 wt %) solution, meaning that the values of k_1 and k_2 have become closer to each other. If the catalysis of the neighboring amic acids are effective in 7.5% solution, it is likely to change the values of k_1 and k_2 in such a way that the value of r is no longer the same as when there is only an electronic effect. In solid films, the catalytic effect may completely overshadow the electronic effect, at least before the film is vitrified, thus leading to an r value greater than 0.3. This possibility would be consistent with the experimentally observed trends in the value of r.

The deconvolution of the UV–visible spectra with three species (PAA, PAI, PII) was carried out to obtain the composition of each species as a function of reaction time. The maximum deconvolution error in the composition of the reacted species in the solid film could be ±10%. Figure 9 illustrates the results obtained at 150 °C. In contrast to Figure 5, which corresponds to the reacted composition of solution imidization, we observe a much faster increase in the concentration of the diimide species (z) in Figure 9, but it levels off at about 53% after 500 min of reaction. The concentration of amic acid/imide decreases while the diimide is increasing, but it also levels off at 20% after only 100 min. The concentration of diamic acids (x) at 5-min reaction time is 60% but becomes about 20% after 500 min of reaction. In Figure 1a, corresponding to the $k_1 = k_2$ case, the experimental data show [AI] decreases much faster
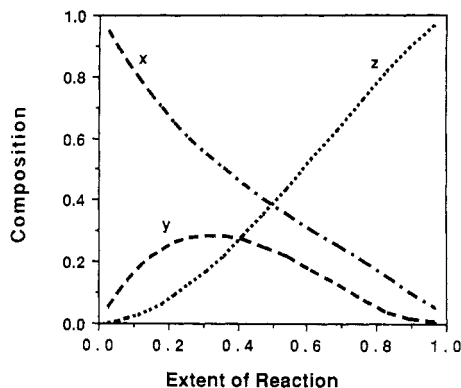
Figure 10. Theoretical prediction of the composition of the imidization species as a function of overall extent of reaction (ξ) according to eq 9–11 for $r = 1$.
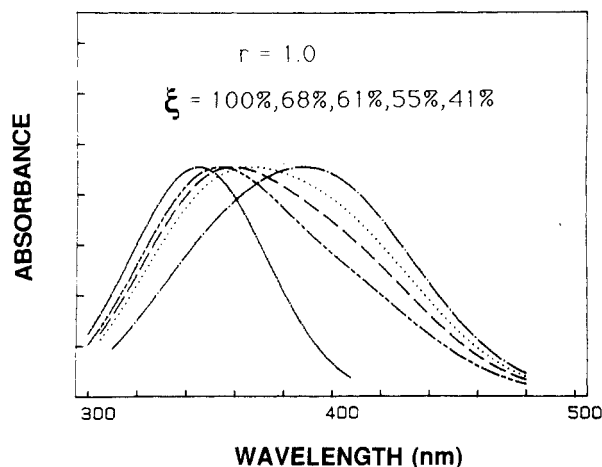

Figure 11. Theoretically generated UV–vis spectra according to eq 9–11 for $r = 1$.

than [AA]. However, with only first-order kinetics the theoretical plots, even with larger r values, do not quite simulate curves like the experimental plot. In addition, predicted spectra show much wider band widths in comparison to the actual spectra show shown Figure 8. Our first approach was to try to take into account the decreasing catalytic effect as the reaction was occurring.

In order to simulate the catalytic effect, we used the following set of kinetic equations:

$$-dx/dt = -2k_1x^2 \tag{9}$$

$$-dy/dt = -2k_1x^2 + k_2y \tag{10}$$

$$-dz/dt = -k_2y \tag{11}$$

As a first approximation, we used second order for the first step, followed by a first-order reaction for the second step to account for the decrease in the concentration of the catalytic amic acid group. A reduced mobility due to the rising glass transition of the matrix film would also decrease the changes for the catalytic group to be in a favorable conformation in the second step. Among several r values tried, the predicted value seems to simulate the results reasonably well when r was approximately 1 (Figure 10). The predicted spectra from these kinetic expressions and r values are shown in Figure 11. The band widths become narrower than in Figure 2a. However, it is still broader than actual experimental spectra, meaning that the above approach does not exactly simulate the kinetic features.

For the 170 and 190 °C solid-state reaction, we do not have enough data points to obtain reliable values of k_1 and
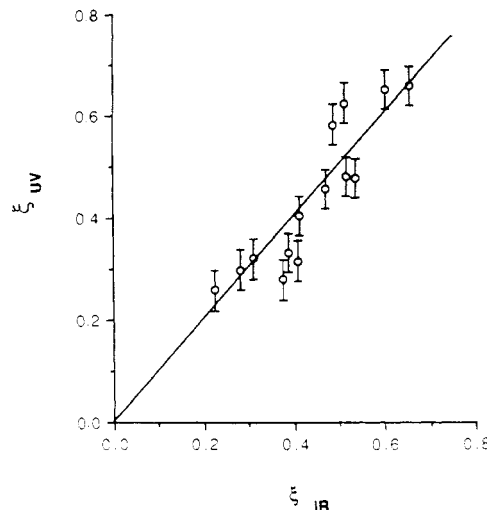

Figure 12. Plot of the extent of reaction (ξ) by UV–vis analyses versus extent of reaction (ξ) by IR analysis for the solid-state reaction at 150 °C.

k_2 before the leveling off since the reaction is much faster. For the 150 °C solid-state reaction, we were not able to determine k_1 and k_2 accurately because the error in the deconvolution was sufficiently large as to render determination of the rate constants inaccurate.

IR Studies and Comparison with UV–Vis Studies. In order to compare the extent of reaction measured by UV–vis studies with other techniques, we carried out IR studies with solid films at 150 °C. In IR studies, the absorption ratio of $A_{721\text{cm}^{-1}}$ due to an imide ring divided by an aromatic internal standard peak at 1015 cm^{-1} has been used to represent a relative imide ring concentration. Then we needed to use this value to calculate the overall extent of reaction. In the past, other researchers assumed that imidization would be complete after a certain reaction condition (e.g., 300 °C for 1 h) was achieved and calibrated the extent of reaction based on the absorbance ratio after the sample was subjected to that condition. We found this procedure to be unsatisfactory because the absorbance ratio would change upon additional reaction time even at high temperatures. Similar trends have been found by Young.[18] Therefore, we used data from one of our UV–vis studies to calibrate the extent of reaction for IR data. For example, the UV–vis data after 1410 min at 150 °C is quite easy to deconvolute. Its extent of reaction, $(\xi_i)_{\text{UV–vis}}$ is 66%. We assume that value to be equal to $(\xi_i)_{\text{IR}}$ under the same reaction condition and scale the IR absorbance ratios accordingly. Figure 12 shows the plot of the extent of overall reaction, $(\xi_i)_{\text{UV–vis}}$ as measured by UV–vis studies according to eq 6 versus the extent of overall reaction $(\xi_i)_{\text{IR}}$ measured by IR studies. Within experimental errors, the data points in general indicate that the two values are similar, as shown by the closeness of the data points to the straight line which corresponds to the $(\xi_i)_{\text{UV–vis}} = (\xi_i)_{\text{IR}}$ case.

Summary

The objective of this paper is to characterize the kinetic parameters and the mechanisms of the imidization process occurring both in solution and in the solid state. Before elaborating on the main tool used in this study, namely, UV–vis spectroscopy, we reviewed the chemistry of polyimides and the results of imidization studies by other spectroscopic techniques in order to illustrate the problems associated with the imidization process and its characterization. In this review, we propose a reaction scheme (Scheme II) for the polyimide synthesis showing various competing reactions and a two-step imidization process as

being representative of cases involving conjugated diamines. We also show that previously used techniques such as IR and NMR failed to differentiate between several imidization species proposed in Scheme II.

In order to accomplish such a differentiation, UV–vis spectroscopy was chosen since various cure species show sensitive changes in the spectral shifts and extinction coefficients, due to the electronic effects of different substituents. For the polyimide system to be used, a conjugated diamine (*p,p'*-diaminoazobenzene) and a nonconjugated dianhydride were chosen to reduce the charge-transfer complex whose intense color could interefere with the UV–vis spectra.

First modeling studies were carried out to predict how the kinetic parameters could influence the spectral changes, assuming two main imidization reactions and neglecting other competing reactions. This is necessary because the first imide ring closure results in a red shift while the second imide ring closure results in a blue shift. Therefore, the overall spectral changes are expected to be a function of the ratio of the two imidization rate constants. The main result of the modeling studies is that two trends are observed depending on the magnitude of the reactivity ratio (r). When r is greater than 0.3, only a blue shifts is predicted. When r is less than 0.3, a red shift is initially predicted followed by a blue shift. However, when r is less than 0.001, a maximum red shift of 24 nm is predicted prior to a blue shift.

During the early stages of imidization in dilute solution, IR analysis suggests some dissociation of polyamic acid as well as imidization. In 1% *N*-methylpyrrolidone solution, the dissociation and the first imide ring closure proceed faster than the second imide ring closure of polyamic acid/imide at all three temperatures studied (150, 170, and 190 °C). This trend is attributed to the reduced basicity of the amide group in polyamic acid/imide in comparison to the analogous group in polyamic acid. Activation energies for the first process and the second ring closure were obtained to be 11 and 18 kcal/mol, respectively. Based on these findings, a mechanism of imidization for dilute solution has been proposed. This two-step imidization is also expected to occur in dilute solution with other conjugated diamines. In fact, we observed similar behavior when 1,5-naphthylenediamine is used for 6F-DA.[19] In a 7.5 wt % solution of NMP, the two rates are not as far apart as in a 1% solution, because of the combination of the electronic and catalytic effects of the neighboring amic acid groups. In solid-state imidization, the apparent imidization rate was initially faster than in dilute solution due to the catalytic effect but levels off probably due to vitrification. Modeling studies to predict spectral changes as a function of the ratio of the two imidization rate constants are consistent with the observed results in dilute solution. The results are adequately modeled by assuming a first-order, two-step imidization reaction. On the other hand, solid film results seem to be reasonably simulated by assuming a second-order reaction for the first step,

followed by a first-order reaction for the second step in order to account for the decrease in the concentration of the conformationally favorable catalytic amic acid group. Finally, there is a good correlation between UV–vis results and IR results in regards to the overall extent of reaction in solid film.

Registry No. (DAA)(6F-DA) (copolymer), 108057-57-4; PAA, 117827-87-9.

References and Notes

(1) (a) Mittal, K. L. *Polyimides, Syntheses, Characterization and Applications*: Plenum: New York, 1984; Vols. I and II. (b) Bessonov, M. I.; Koton, M. M.; Kudryavtsev, V. V.; Laius, L. A.; translated by Wright, W. W. *Polyimides, Thermally Stable Polymers*; Consultants Bureau; New York, 1987.

(2) (a) Kreuz, J. A.; Endrey, A. L.; Gay, F. P.; Sroog, C. E. *J. Polym. Sci., Part A-1* **1966**, 2607. (b) Lavrov, S. V.; Kardash, I. E.; Pravednikov, A. N. *Polym. Sci. U.S.S.R.* **1977**, *19*, 2727. (c) Lavrov, S. V.; Ardashnikov, A. Y.; Kardash, I. E.; Pravednikov, A. N. *Polym. Sci. U.S.S.R.* **1977**, *19*, 1212.

(3) Mathisen, R. J.; Yoo, J. K.; Sung, C. S. P. *Macromolecules* **1987**, *20*, 1414.

(4) (a) Koton, M. M.; Kudriavtsev, V. V.; Svetlichny, V. M., ref. 1a, Vol. 1, p 171. (b) Kaas, R. L. *J. Polym. Sci., Polym. Chem. Ed.* **1981**, *19*, 2255.

(5) (a) Kardash, I. E.; Ardashnikov, A. Y.; Yukushin, F. S.; Pravednikov, A. N. *Polym. Sci. U.S.S.R.* **1975**, *A17*, 598. (b) Gay, F. P.; Berr, C. E. *J. Polym. Sci., Part A-1* **1968**, *6*, 1935.

(6) Sroog, C. E.; Endrey, A. L.; Abramo, S. V.; Berr, C. E.; Edwards, W. M.; Olivier, K. L. *J. Polym. Sci., A1* **1965**, *3*, 1373.

(7) Brekner, M. J.; Feger, C. *J. Polym. Sci., Polym. Chem. Ed.* **1987**, *25*, 2479.

(8) Ginsburg, R.; Susko, J. R., ref 1a, Vol. 1, p 237.

(9) Palmese, G. R.; Gillham, J. K. *ACS PMSE Proc.* **1986**, *55*, 390.

(10) Baise, A. I. *J. Appl. Polym. Sci.* **1986**, *32*, 4043.

(11) Laius, L. A.; Tsapovetsky, M. I., ref 1a, Vol. 1, p 295.

(12) Weber, W. D.; Murphy, P. D. *ACS PMSE Proc.* **1987**, *57*, 341.

(13) (a) Dine-Hart, R. A.; Wright, W. W. *Makromol. Chem.* **1971**, *143*, 189. (b) Gordina, T. A.; Kotov, B. V.; Kolnivov, O. V.; Pravednikow, A. N. *Vysokomol. Soed.* **1973**, *B15*, 378.

(14) Kotov, B. V.; Gordina, T. A.; Voischchev, V. S.; Kolninov, O. V.; Pravednikow, A. N. *Vysokomol. Soed.* **1977**, *A19*, 614.

(15) Sung, C. S. P.; Pyun, E.; Sun, H.-L. *Macromolecules* **1986**, *19*, 2922.

(16) Bublik, L. S.; Motseev, V. D.; Chernova, A. G.; Pilyaeva, V. P.; Nekrasova, L. P. *Plast. Massy* **1974**, *No. 3*, 10.

(17) Kamzolkina, E. V.; Nechaev, P. P.; Markin, V. S.; Vygodskii, Y. S.; Grigoreva, T. V.; Zaikov, G. E. *Dokl. Akad. Nauk SSSR* **1974**, *219*, 650.

(18) Young, P. Private communications, 1987.

(19) Dickinson, P.; Sung, C. S. P. *ACS Polym. Prepr.* **1988**, *29-1*, 530.